



Deletion of cystathionine- γ -lyase in bone marrow-derived cells promotes colitis-associated carcinogenesis

Ketan K. Thanki^{a,1}, Paul Johnson^{a,1}, Edward J. Higgins^a, Manjit Maskey^a, Ches'Nique Phillips^a, Swetaleena Dash^a, Francisco Arroyo Almenas^a, Armita Abdollahi Govar^a, Bing Tian^b, Romain Villéger^{b,2}, Ellen Beswick^c, Rui Wang^d, Csaba Szabo^e, Celia Chao^a, Irina V. Pinchuk^{b,3}, Mark R. Hellmich^{a,**}, Katalin Módis^{a,*}

^a Department of Surgery, University of Texas Medical Branch, Galveston, TX, USA

^b Department of Internal Medicine, University of Texas Medical, Galveston, TX, USA

^c Department of Internal Medicine, Huntsman Cancer Institute, University of Utah, Salt Lake City, UT, USA

^d Department of Biology, York University, Toronto, ON, Canada

^e Chair of Pharmacology, Section of Science and Medicine, University of Fribourg, Fribourg, Switzerland

ARTICLE INFO

Keywords:

Inflammatory bowel disease
Colorectal cancer
Hydrogen sulfide
Transsulfuration pathway
Ulcerative colitis
Bone marrow

ABSTRACT

Ulcerative colitis (UC) is characterized by widespread relapsing inflammation of the colonic mucosa. Colitis-associated cancer (CAC) is one of the most serious complications of a prolonged history of UC. Hydrogen sulfide (H₂S) has emerged as an important physiological mediator of gastrointestinal homeostasis, limiting mucosal inflammation and promoting tissue healing in response to injury. Inhibition of cystathionine- γ -lyase (CSE)-dependent H₂S production in animal models of UC has been shown to exacerbate colitis and delay tissue repair. It is unknown whether CSE plays a role in CAC, or the downregulation of CSE expression and/or activity promotes CAC development.

In humans, we observed a significant decrease in CSE expression in colonic biopsies from patients with UC. Using the dextran sodium sulfate (DSS) model of epithelium injury-induced colitis and global CSE KO mouse strain, we demonstrated that CSE is critical in limiting mucosal inflammation and stimulating epithelial cell proliferation in response to injury. *In vitro* studies showed that CSE activity stimulates epithelial cell proliferation, basal and cytokine-stimulated cell migration, as well as cytokine regulation of transepithelial permeability. In the azoxymethane (AOM)/DSS model of CAC, the loss of CSE expression accelerated both the development and progression of CAC. The increased tumor multiplicity and severity of CAC observed in CSE-KO mice were associated with reduced levels of mucosal IL-10 expression and increased levels of IL-6. Restoring CSE expression in bone marrow (BM) cells of CSE-KO mice through reciprocal BM transplantation raised mucosal IL-10 expression, decreased IL-6 level, and reduced the number of aberrant crypt foci and tumors in AOM/DSS-treated mice.

These studies demonstrate that CSE expression in BM cells plays a critical role in suppressing CAC in mice. Furthermore, the data suggest that the inhibitory effects of CSE on the development of CAC are due, in part, to the modulation of mucosal pro- and anti-inflammatory cytokine expression.

* Corresponding author. The University of Texas Medical Branch at Galveston, 301 University Blvd, Galveston, TX, 77555, USA.

** Corresponding author. The University of Texas Medical Branch at Galveston, 301 University Blvd, Galveston, TX, 77555, USA.

E-mail addresses: kkthanki@gmail.com (K.K. Thanki), pjohnson08.2012@gmail.com (P. Johnson), Edward.higgins1@gmail.com (E.J. Higgins), mamaskey@utmb.edu (M. Maskey), cphil1@lsuhsc.edu (C. Phillips), swetaleena.dash@outlook.com (S. Dash), farroyo10@yahoo.com (F.A. Almenas), armita.lsu@gmail.com (A.A. Govar), bitian@utmb.edu (B. Tian), romain.villeger@univ-poitiers.fr (R. Villéger), ellen.beswick@hsc.utah.edu (E. Beswick), ruiwang@yorku.ca (R. Wang), csaba.szabo@unifr.ch (C. Szabo), cchao986@gmail.com (C. Chao), ipinchuk@pennstatehealth.psu.edu (I.V. Pinchuk), mhellmic@utmb.edu (M.R. Hellmich), kamodis@utmb.edu (K. Módis).

¹ These authors contributed equally to this work.

² Laboratoire Ecologie & Biologie des Interactions, UMR CNRS 7267 Université de Poitiers, 86,000 Poitiers, France.

³ Mechanisms of Carcinogenesis Program, Division of Gastroenterology, Department of Medicine, Penn State Health Milton S. Hershey Medical Center, Penn State Cancer Institute, Pennsylvania State University College of Medicine, Hershey, PA 17033, USA.

<https://doi.org/10.1016/j.redox.2022.102417>

Received 9 May 2022; Received in revised form 27 June 2022; Accepted 17 July 2022

Available online 21 July 2022

2213-2317/Published by Elsevier B.V. This is an open access article under the CC BY-NC-ND license (<http://creativecommons.org/licenses/by-nc-nd/4.0/>).

1. Introduction

Abbreviations:

ACF	Aberrant Crypt Foci
AOM	azoxymethane
BM	Bone Marrow
CAC	Colitis-Associated Cancer
CRC	Colorectal Cancer
CBS	Cystathionine- β -synthase
CSE	Cystathionine- γ -lyase
DSS	Dextran Sulfate Sodium salt
GI	Gastrointestinal
HCEC	Human Colon Epithelial Cell
H ₂ S	Hydrogen Sulfide
IBD	Inflammatory Bowel Disease
KO	Knock-out
PAG	DL-propargylglycine
TEER	Trans-Epithelial Electrical Resistance
TNBS	Trinitrobenzene Sulfonic Acid
TSP	Transsulfuration Pathway
UC	Ulcerative Colitis

Colon cancer is one of the most severe complications of chronic inflammatory bowel diseases (IBD), particularly in long-duration ulcerative colitis (UC). The cumulative probability of developing colitis-associated cancer (CAC) ranges from 2% for patients with a 10-year history of UC to 18% for those with symptoms for 30 years or more [1]. The incidence is four to ten times greater than sporadic colon cancer, and the average age of onset is 20 years earlier [2–4]. Once formed, CAC often progresses rapidly and is resistant to most current therapeutic regimens, resulting in high mortality [5]. Addressing this significant health challenge with novel treatment strategies requires a better understanding of the basic cellular and molecular mechanisms mediating CAC development.

It is well-known that chronic inflammation predisposes one to the development of cancer [6,7]. In inflammatory bowel diseases (IBD), such as UC, repetitive cycles of acute inflammation coupled with insufficient resolution, create a pro-neoplastic milieu characterized by excessive tissue damage, dysregulated healing, and abnormal epithelial cell proliferation, suggesting that CAC arises from a failure of the normal physiological mechanisms mediating intestinal immune homeostasis and tissue repair [8].

The gasotransmitter hydrogen sulfide (H₂S), has emerged as an important mediator of gastrointestinal (GI) homeostasis, functioning to limit mucosal inflammation and promote healing in response to epithelial injury [9–16]. A major source of endogenous H₂S in mammalian cells is the transsulfuration pathway (TSP) enzymes: cystathionine- β -synthase (CBS) and cystathionine- γ -lyase (CSE). CBS is the rate-limiting enzyme in the TSP, converting homocysteine, derived from the methionine cycle, to cystathionine, which in turn, is converted to L-cysteine by CSE. Both, pyridoxal 5'-phosphate (vitamin B6)-dependent enzymes use L-cysteine and other TSP intermediates as substrates to produce H₂S through various elimination and condensation reactions [17,18].

Experimental animal models have revealed a critical role for TSP enzymes and H₂S in reestablishing gastrointestinal mucosal integrity following an inflammatory insult [19–23]. Wallace *et al.* reported a significant increase in H₂S production in rat colon tissue homogenates after initiating hapten-induced acute colitis with trinitrobenzene sulfonic acid (TNBS) [23]. Hirata *et al.* showed a time-dependent induction

of colonic H₂S production, as well as increased expression of both CSE and CBS mRNA following dextran sodium sulfate (DSS)-induced acute mucosal injury [21]. Moreover, Flannigan *et al.* reported increased levels of H₂S production specifically at sites of mucosal ulcerations in a rat model of chronic dinitrobenzene sulfonic acid (DNBS)-induced colitis [20]. Importantly, inhibiting the induction of TSP-dependent H₂S production in these experimental models with enzyme-selective pharmacological inhibitors, vitamin B6 deficient diet, or targeted TSP enzyme deletion exacerbated the clinical and histological indices of colitis, increased plasma homocysteine levels (i.e., hyperhomocysteinemia), and delayed mucosal healing [19–23], suggesting that downregulation of TSP activity could lead to a chronic inflammatory state, and thus, an increased risk of CAC.

This supposition is supported, in part, by human clinical studies showing that patients with IBD are more likely to have hyperhomocysteinemia [24–28]. Approximately 28% of IBD patients showed increased plasma level of homocysteine compared to 3–10% of patients without IBD. In a meta-analysis of 28 clinical studies, Oussalah *et al.* determined that the risk of hyperhomocysteinemia was significantly higher in patients with IBD than in the general population (odds ratio = 4.65, 95% CI, 3.04–7.09; $p < 0.0001$) [25]. Additionally, Chen *et al.* have recently documented significantly lower levels of CBS protein expression in surgically resected colon specimens from UC patients, compared to biopsies of histologically normal colon mucosal, suggesting downregulation of TSP activity in these patients [29]. Finally, hyperhomocysteinemia is also associated with an increased risk of developing both adenomatous polyps and CRC [30,31]. Together these studies suggest a potential mechanistic link between downregulated TSP activity, chronic inflammation, and colon carcinogenesis.

This study aimed to determine whether decreased TSP activity, specifically loss of CSE, could alter the pathogenesis of experimental CAC. Using the mutagen azoxymethane (AOM) in combination with the DSS model of injury-induced colitis in mice, we demonstrate that loss of CSE expression in bone marrow (BM)-derived cells, alters the balance of mucosal IL-6 and IL-10 expression and accelerates the development and progression of CAC. Using a normal human colonic epithelial cell line, we show that CSE activity and H₂S regulate key cellular processes involved in both colonic epithelium restitution and proliferation, processes critical for the normal tissue repair and maintenance of mucosa integrity. Together our findings suggest that CAC may result from a failure of the normal physiological mechanisms mediating intestinal immune homeostasis and tissue repair regulated by CSE and H₂S.

2. Materials and methods

Chemicals. The H₂S donor GYY4137 (GYY), DL-propargylglycine (PAG), azoxymethane (AOM), hydrocortisone, insulin, transferrin, L-cysteine, pyridoxal phosphate (PLP), bovine serum albumin (BSA), and sodium selenite were obtained from Sigma-Aldrich (St. Louis, MO, USA). Dextran sulfate sodium salt (DSS) MW ca 40,000 was purchased from Alfa Aesar (Haverhill, MA, USA).

Human Tissue. Colon mucosal samples were obtained from patient biopsies and discarded tissue from colorectal resections in compliance with protocols approved by the University of Texas Medical Branch Institutional Review Board (IRB). Vulnerable populations (e.g., age less than 18) were not included in the study.

Mice. The CSE gene knockout (CSE-KO) mouse is an inbred strain (C57BL/J6; 129SvEv) developed by Dr. Rui Wang. The gene deletion was achieved by replacing 5.5 kb of exons 1–3 with a 1.8 kb neomycin resistance gene cassette, as previously described [32]. The CSE deficient mice exhibited increased plasma levels of homocysteine and reduced levels of cysteine and H₂S compared to WT animals. The CSE-KO and B6129F2 hybrid wild-type (WT) control mice (Jackson Laboratory, Bar Harbor, ME, USA) were co-housed in a non-sterile, temperature-controlled environment under a 12-h day/night light cycle and maintained on a diet of standard rodent chow and regular drinking

water *ad libitum*. All experiments were performed under an Institutional Animal Care and Use Committee (IACUC) approved protocols at the University of Texas Medical Branch.

Human Colon Epithelial Cell Line. The human colon epithelial cell (HCEC) line was provided by Dr. Jerry Shay, University of Texas Southwestern, Dallas, TX. The HCECs were derived from a histologically normal colonic tissue biopsied from a patient undergoing routine colonoscopy screening. The cells were immortalized with ectopic expression of cyclin-dependent kinase 4 (CDK4) and human telomerase reverse transcriptase (hTERT) [33]. To maintain a stable normal karyotype (i.e., 46, XY), HCECs were continuously cultured in Primaria flasks (BD Biosciences, San Jose, CA, USA) in high-glucose Dulbecco's Modified Eagle Media (DMEM, Sigma-Aldrich) supplemented with 2% Cosmic Calf Serum (Hyclone, GE Healthcare Bio-Sciences, Pittsburg, PA, USA), EGF (25 ng/ml) (PeproTech Inc, Rocky Hill, NJ, USA) hydrocortisone (1 µg/ml), insulin (10 µg/ml), transferrin (2 µg/ml), sodium selenite (5 nM), gentamicin sulfate (50 µg/ml) (Gemini Bio-Products, West Sacramento, CA, USA), and under a humidified atmosphere of 2% oxygen/5% carbon dioxide at 37 °C.

Acute Colitis Model. To induce acute experimental colitis, we used DSS, a chemical colitogen that causes inflammation by disrupting the colonic epithelium barrier allowing luminal bacteria and associated antigens to penetrate the underlying tissue [34]. CSE-KO and WT mice [matched for age (10–12 weeks) and sex] were given 2% (w/v) DSS in their drinking water for 7 days. To inhibit CSE activity in WT mice, animals were injected daily with PAG (10 mg/kg, 100 µL IP) or the equivalent volume of sterile PBS. On day 8, mice were anesthetized with ketamine/xylazine [80 mg/kg/10 mg/kg, intraperitoneal (IP) injection], euthanized by cervical dislocation, and tissues collected for analyses.

Colitis-associated Cancer (CAC) Model. To induce CAC, we treated mice with a combination of azoxymethane (AOM) and DSS. AOM is a carcinogen that causes O⁶-methylguanine adducts in DNA, leading to G→A transitions and tumorigenesis in the distal colon of experimental animals. On Day 0, all mice received a single IP injection of AOM [10 mg/kg in phosphate buffered saline (PBS)] and were then separated into age- and sex-matched groups of 10 mice each to receive 1, 2, or 3 cycles of DSS-induced colitis. Each cycle of colitis involved 7 days of exposure to DSS (2%, w/v) dissolved in the drinking water, followed by 14 days of regular water. On Day 21, 42, 63, and 80 colons were collected for analyses.

Tissue Processing. The colons were cut open longitudinally, spread out on a glass slide to reveal the mucosal surface, washed with PBS and photographed with a high-definition camera. For colons harvested on days 42, 63, and 80, tumors were identified at 4× magnification using a dissection microscope. For colons collected on day 21, the tissue was fixed in 10% formalin (24 h), transferred to 70% ethanol, and stained with 0.05% methylene blue dye. After flattening the tissue between a slide and glass coverslip, aberrant crypt foci (ACF) and/or microscopic tumors were counted at 200X and 40× magnification, respectively. The percentage of tumor area per colon (i.e., tumor burden) was calculated using the formula: [(sum of the area of all individual tumors ÷ total area of the colon) x 100]. Areas were measured using ImageJ software [35]. Colon tissues were also prepared for histological inflammation scoring and immunohistochemical analyses using the Swiss roll technique [36]. Finally, tissue protein homogenates and total RNA extracts were prepared from colon mucosal scrapings, snap-frozen in liquid nitrogen, and used either for TPS enzyme activity assays (i.e., H₂S production), Western blotting or Reverse Transcription-quantitative Polymerase Chain Reaction (RT-qPCR) assays.

Inflammatory Score. Formalin-fixed paraffin-embedded colon Swiss rolls were sectioned (5 µm), deparaffinized in three changes of xylene for 5 min each, rehydrated, and stained with hematoxylin and eosin (H&E). The H&E-stained tissue sections were examined in their entirety under low (40X) and high (100X & 200×) magnifications and scored for inflammation using a five-category, nine-point system modified from

Geboes et al., 2000 [37]. Scoring was performed independently by 3 investigators (K-K.T, P.J, I-V.P) blinded to the identity of the groups.

H₂S Measurements. H₂S levels were determined using 7-azido-4-methylcoumarin (AzMC), a fluorescent probe (Adipogen-Chemodex, San Diego, CA). Colonic mucosal scrapings or cell pellets were lysed in a solution containing 50 mM Tris-HCl (pH 8.0), 150 mM NaCl, 1% NP-40, and supplemented with protease and phosphatase inhibitors. Protein concentrations of lysates were determined with Pierce BCA Protein Assay reagents. To measure enzyme-produced H₂S, protein extracts (200 µg/ml) were incubated with L-cysteine (10 mM), PLP (0.005 mM), and AzMC (0.01 mM) at 37 °C for 1 h. The fluorescence signal was measured using a SpectraMax M2 (Molecular Devices, San Jose, CA, USA) microplate reader (excitation λ = 365, emission λ = 450 nm).

Proliferation Assay. HCECs were plated in 6 well plates (10⁴ cells/well) and incubated at 37 °C for 12, 24, 48, 72, or 96 h. Cell number was assessed at each time point using a Z-Series Coulter Cell Counter (Beckman-Coulter Biotechnology, Brea, CA, USA), as previously described [38]. CSE enzyme activity was inhibited by treating cultures every second day with PAG dissolved in PBS. Control cultures were treated on the same schedule with an equivalent volume of PBS (vehicle).

Migration Assay. HCECs suspended in DMEM containing 0.1% bovine serum albumin (BSA) were seeded (10⁵ cells/well) into the upper chambers of 8-µm transwells (Corning, Tewksbury, MA). The bottom chambers contained 0.6 ml of NIH3T3 fibroblast-conditioned medium. For cytokine-stimulated migration experiments, the cytokine (i.e., TNF-α or IL-10) was added at the same final concentration to both the top and bottom chambers of the transwell. Cell migration was quantified following incubation periods of 6, 12, or 18 h at 37 °C (5% CO₂). Cells that migrated through the transwell membrane were fixed with methanol and then stained with 0.1% crystal violet [38]. Stained cells were counted in a minimum of five non-overlapping fields at 200× magnification for each transwell insert by 4 investigators (K-K.T, C. Philips, E.J. H, S.D.) blinded to the identity of the groups.

Measurement of Trans-Epithelial Electrical Resistance (TEER). HCECs were grown in 24-well ThinCert™ transwell plates (Greiner Bio-One, Monroe, NC, USA), coated with type 1 collagen for 6 days or until the TEER measurements reached ~400 Ohms (Ω). Cultures were pre-treated for 2 h with PAG (3 mM) followed by TNF-α (1 or 10 ng/ml) or sterile PBS (vehicle control). TEER was measured using an EVOM2™ VoltOhmmeter (World Precision Instruments, Sarasota, FL, USA) every 2 h for the first 10 h and then at 18 and 24 h after the addition of TNF-α.

Immunohistochemical Staining. Formalin-fixed paraffin-embedded colon sections (5 µm) were deparaffinized in xylene and rehydrated through a step-gradient of ethanol solutions. Antigen retrieval was performed by incubating the sections in 0.01 M citrate buffer (pH 6.0) for 20 min at 98 °C, followed by 20 min at room temperature (RT) in the same solution. Endogenous peroxidase activity was inhibited with 3% H₂O₂ (in deionized water) at RT for 15 min. For Ki67 staining, tissue sections were blocked for 10 min with Background Sniper (Biocare Medical, Pacheco, CA, USA), incubated with rat monoclonal Ki67 antibody (1:250 dilution, eBioscience, San Diego, CA, USA) overnight at 4 °C, followed by a goat anti-rat (Invitrogen, Carlsbad, CA, USA) secondary antibody for 1 h at RT. For CSE immunostaining, tissue sections were blocked for 30 min with 5% goat serum (Vector Laboratories, Burlingame, CA, USA), incubated with rabbit polyclonal CSE antibody (1:150 dilution, Proteintech, Rosemont, IL, USA) for 1 h at RT, and then a goat anti-rabbit (Vector Laboratories) secondary antibody for 1 h at RT. The non-specific background binding of each primary antibody was determined by immunostaining a serially cut tissue section with an isotype-matched immunoglobulin control at the same dilution as the primary antibody. Immunostaining was detected with 3,3'-diaminobenzidine (DAB). Images were captured using an Olympus BX51 microscope following dehydration of the stained sections through a step-gradient of ethanol solutions and finally, xylene.

Western Blotting. Protein extracts for immunoblots were prepared

by homogenizing mucosal scrapings (1 mg wet weight tissue per ml) or cell pellets with either a Dounce glass-on-glass homogenizer (tissue) or a polypropylene pestle (cells) in a solution containing 50 mM Tris-HCl, pH 8.0 and 1% NP-40 (v/v) supplemented with protease and phosphatase inhibitors (Protease and Phosphatase Inhibitor Mini Tablets, ThermoFisher). The protein concentrations of samples were quantified using the Pierce BCA Protein Assay (ThermoFisher) and bovine serum albumin (BSA) as a standard. Proteins were resolved on 4–12% Bis-Tris gradient gels (Invitrogen) and transferred to PVDF membranes using a Pierce Power Blotter. Membranes were blocked with StartingBlock™ blocking buffer and then incubated overnight at 4 °C with a primary antibody either to CSE (Proteintech, Cat.# 12217-1-AP) or CBS (Proteintech, Cat.# 14787-1-AP). Membranes were washed three times with Tris-buffered saline containing 1% Tween detergent (TBST) and incubated for 1 h at RT with a horseradish peroxidase-conjugated secondary antibody. Enhanced chemiluminescent substrate (Thermo Fisher) was used to detect the signal in a camera-based chemiluminescence detection system (Alpha Innotech MultiImage II Alphaimager HP, ProteinSimple, San Jose, CA). Immunostaining for GAPDH or β -actin was used to normalize protein expression levels. Densitometry was performed using ImageJ software.

Bone Marrow (BM) Transplant. Reciprocal BM cell transplants were performed between CSE-KO and WT mice. Bone marrow cells were isolated from the femurs and tibias of donor mice (age 5–7 weeks) and injected (2×10^6 in 100 μ L) into the retroorbital sinus of recipient mice (age 10–12 weeks) exposed to a lethal dose of radiation (10 Gy) using a cesium (Cs-137) source. All recipient mice were pretreated with antibiotics for 5 days prior to irradiation, kept in sterile cages, and given antibiotics for two weeks following exposure to irradiation. Colitis-associated carcinogenesis was induced as described above. Colon tissue was harvested on day 21 post AOM injection. This experiment was repeated 4 times. For each repeat, a set ($n = 2$) of control WT and CSE-KO mice were irradiated but not transplanted to ensure lethality of the radiation exposure.

Reverse Transcription-quantitative Polymerase Chain Reaction (RT-qPCR) Assay. Total RNA was extracted from HCEC or colon mucosal scrapings using RNAqueous™ (Life Technologies) and quantified using a NanoDrop ND-1000. Quality was assessed by visualization of 18S and 28S RNA bands using an Agilent BioAnalyzer 2100; electropherograms were used to calculate the 28S/18S ratio and the RNA integrity number. Reverse transcription to cDNA was performed using the Applied Biosystems cDNA synthesis kit (Foster City, CA). The appropriate assays-on-demand™ gene expression FAM™ labeled primer/probe mix was purchased from Thermo Fisher Scientific. The following primer sequences were used to amplify human IL-6 (forward AGTGAGGAACAAGCCAGAGCTG and reverse GGCATTTGTGGTTGGGTCAG), mouse IL-6 (forward TAGCTTCC-TACCCCAATTCC and reverse TTGGTCTTAGCCACTCCTTC), human IL-10 (forward ACAAGCAAGGCCGTGG and reverse GAA-GATGTCAAACCTCACTCATGGC), mouse IL-10 (forward GCTCTTACT-GACTGGCATGAG and reverse CGCAGCTCTAGGAGCATGTG) human CSE (forward –ATGTTGTAATGGCCCTGGTGTC and reverse AATCAA-TAGGAGATGGAAGTCTCC), and human TNF- α (forward TTCTCCTCTGATCGTGGC and reverse TGATTAGAGAGAGGTCCC-TGGG). FastStart Universal Probe Master mix (Roche Diagnostic USA, Indianapolis, IN) was used to prepare a PCR mix according to the manufacturer's instruction. The reactions were carried out in a 20 μ L final volume using a BioRad Q5 real-time PCR machine according to the following protocol: 2 min at 50 °C, 10 min at 95 °C (1 cycle) and 15 s at 95 °C and 1 min at 60 °C (40 cycles). The threshold cycle (C_T) value for each gene was normalized to a housekeeping gene (e.g., 18S RNA, GAPDH, β -actin or cyclophilin); relative expression levels were calculated using n-fold change = $2^{-\Delta\Delta C_T}$, where $\Delta\Delta C_T = \Delta C_T$ (target sample) - ΔC_T (control sample).

Statistical Analyses. Statistical analyses were performed using GraphPad Prism 9 (GraphPad Software, La Jolla, CA). Data are expressed as the mean \pm standard error of mean (SEM) unless otherwise indicated. Normal distribution of data was determined using either the

Shapiro-Wilk test or D'Agostino & Pearson test. To analyze normally distributed data, we used either an unpaired t-test (two-tailed), one-way ANOVA or 2-way ANOVA, with either Tukey or Šidák multiple comparison post-hoc tests. For analyses of non-parametric data, we either used the Mann-Whitney test (two-tailed) or Kruskal-Wallis test, with Dunn's multiple comparison post-hoc test. All *in vitro* experiments had a minimum of 3 technical repeats per condition and each experiment was independently repeated a minimum of 3 times. All animal experiments contained 10 mice per group and were repeated a minimum of 3 times.

3. Results

CSE expression is downregulated in human UC specimens. A growing body of clinical evidence suggests that TSP activity may be reduced in patients with IBD [24–29]. To expand on this emerging data, we assessed the relative expression levels of CSE and CBS in biopsy specimens from both healthy individuals undergoing routine screening colonoscopies and from patients with UC. We did not find a significant difference in CBS protein levels between UC specimens and histologically normal colon tissue (Fig. 1A&B). However, we did detect reductions of both CSE mRNA (34% decrease, $p < 0.05$) (Fig. 1C) and protein levels (49% decrease, $p < 0.005$) in UC specimens relative to healthy control samples (Fig. 1D&E). Immunohistochemical staining of formalin-fixed paraffin-embedded tissues sections confirmed an overall lower level of CSE protein expression in the UC specimens (Fig. 1F&G) with reductions noted in both the colonic epithelial cells (Fig. 1G, EpCs) and within cells of the loose connective tissue of the mucosal lamina propria (Fig. 1G, LP).

Effects of CSE gene deletion on DSS-induced colitis. Given the observation of reduced expression of CSE in human UC specimens, we used a mouse bearing a homozygous CSE gene deletion (CSE-KO) [32] to first confirm the function of CSE in acute colitis, and then to assess its role in chronic colitis-associated carcinogenesis. Western blotting confirmed no immunoreactive protein corresponding to CSE (~45 kDa) in protein homogenates from the colonic mucosa of CSE-KO mice, whereas it was readily detectable in the colons of WT mice (Fig. 2A). In contrast to our patient data, CBS protein levels were significantly higher in the colons of CSE-KO mice, compared to WT animals (Fig. 2A). The reason for increased CBS expression in CSE-KO mice is unknown. However, it may be a compensatory feedback response to the reduced CSE-mediated cysteine synthesis. Zhu et al. have recently reported that expression of both CBS and CSE are induced in cysteine deprived cells in culture through a mechanism involving the general control non-depressible 2 (GCN2) and activating transcription factor 4 (ATF4) signaling pathway [39].

We next evaluated how inhibition or loss of CSE affected the course of acute DSS-induced colitis. Both WT and CSE-KO mice showed a significant reduction in body weight following DSS treatment (Fig. 2B). Treatment with the CSE inhibitor PAG caused additional weight loss in DSS-treated WT mice compared to either untreated mice or animals treated with only DSS. The reduction in body weight of WT mice treated with both DSS and PAG was similar in scale to that of CSE-KO animals treated with DSS (i.e., ~15% weight reduction) (Fig. 2B).

Loss of CSE prevents injury-induced increases in mucosal H₂S production and exacerbates inflammation. Following 7 days of DSS-induced injury, WT mice exhibited an approximately 2-fold increase in mucosal H₂S production compared to untreated animals (Fig. 2C, WT + DSS vs. untreated WT; $p < 0.0001$), and the increase in H₂S production was partially inhibited in mice simultaneously receiving DSS in their drinking water and PAG injections (Fig. 2C, WT + DSS + PAG vs. WT + DSS; $p < 0.0001$). In contrast to the untreated WT mice, mucosal homogenates from untreated CSE-KO mice exhibited a significantly lower basal level of H₂S synthesis (Fig. 2C, WT vs. CSE-KO; $p = 0.0315$), despite having a higher level of CBS expression (Fig. 2A) and failed to show induction of H₂S production in response to DSS-induced injury (Fig. 2C). As expected, PAG had no effect on either basal or DSS-induced

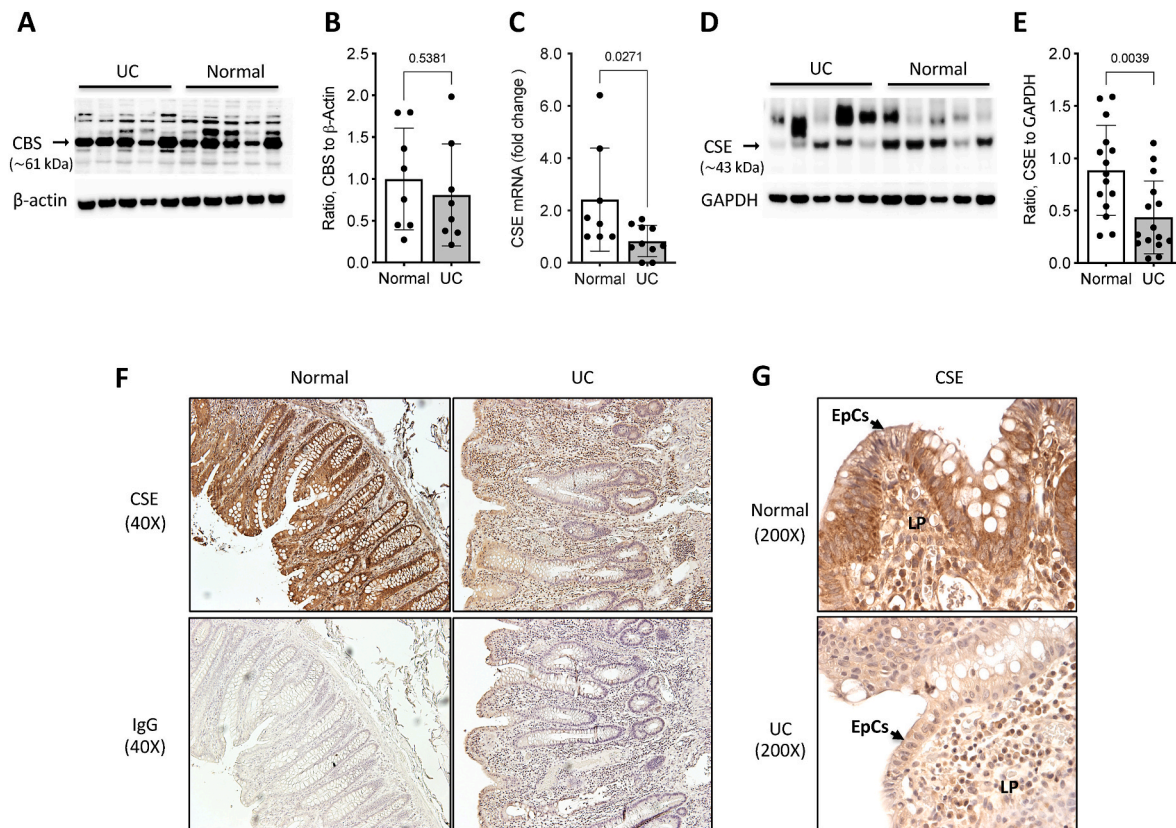


Fig. 1. Mucosal biopsy specimens from patients with ulcerative colitis (UC) show reduced CSE expression. A) Representative Western blot comparing CBS protein expression in colon mucosa biopsies from patients with ulcerative colitis (UC) and healthy individuals (Normal). B) Results of densitometric analysis of CBS expression in UC (n = 8) and normal (n = 8) mucosal specimens. C) Reverse Transcription-quantitative Polymerase Chain Reaction (RT-qPCR) assay comparing CSE mRNA levels in mucosal biopsies from normal and patients with UC. D) Representative Western blot comparing CSE protein levels in colon mucosa biopsies from healthy and UC patients. E) Results of densitometric analysis of CSE expression in UC (n = 14) and normal (n = 14) mucosal specimens. Statistical analyses of data in panels B, C, and E: D'Agostino & Pearson Normality test, Unpair *t*-test, two-tailed, error bars represent standard deviation, p values shown. F&G) Immunohistochemical staining for CSE protein (brown) using formalin-fixed paraffin-embedded tissue sections (5 μ m thickness) from representative healthy and UC biopsy specimens. The sections were counterstained with hematoxylin (purple) to reveal tissue architecture. Non-specific antibody binding was determined by immunostaining serial tissue sections with an isotype-matched rabbit immunoglobulin (IgG) at the same concentration (2 ng/ μ L) as the primary rabbit anti-CSE antibody. Images were taken at 40X (F) and 200 \times (G) magnification (EpCs: epithelial cells; LP: lamina propria). (For interpretation of the references to color in this figure legend, the reader is referred to the Web version of this article.)

colonic H₂S production in CSE-KO animals (Fig. 2C). Together these findings confirm that CSE is an important source of injury-induced H₂S production in the mouse colon.

Consistent with an anti-inflammatory function for H₂S, DSS-treated CSE-KO mice exhibited more severe mucosal inflammation than similarly treated WT mice (Fig. 2D, CSE-KO + DSS vs. WT + DSS, *p* = 0.0002). Furthermore, simultaneous treatment with DSS and a slow-release H₂S donor [GYY4137 (GYY), 100 mg/kg, IP injection, daily] reduced colitis scores in both WT and CSE-KO mice (Fig. 2D, WT + DSS vs. WT + DSS + GYY; *p* = 0.0034, CSE-KO + DSS vs. CSE-KO + DSS + GYY; *p* < 0.0001), corroborating previous studies showing that exogenous H₂S donors can reduce the severity of acute inflammation [13,20].

Loss of CSE inhibits injury-induced epithelial cell proliferation. Colon epithelial cell proliferation was assessed by immunostaining formalin-fixed paraffin-embedded mouse tissue sections for the nuclear antigen Ki67 before and after a 7-day exposure to DSS drinking water. Colons from untreated WT and CSE-KO mice exhibited similar numbers of Ki67 positive epithelial cells per colonic crypt (Fig. 2E, WT Control vs. CSE-KO Control; *p* > 0.99). However, following DSS treatment, only WT mice showed a significant increase in the number of Ki67-positive epithelial cell nuclei per crypt when compared either to untreated WT animals (Fig. 2E, WT + DSS vs. WT Control; *p* = 0.0015) or DSS-treated CSE-KO mice (Fig. 2E&F, WT + DSS vs. CSE-KO + DSS; *p* = 0.0255), suggesting that CSE activity is necessary to promote colonic epithelial

cell proliferation in response to injury *in vivo*.

CSE promotes human colon epithelial cell (HCEC) proliferation *in vitro*. To examine whether CSE regulates cell proliferation in a cell-autonomous manner, we treated normal human colonic epithelial cells (HCECs) in culture with different concentrations of PAG (Fig. 3A) or transfected them with a siRNA targeting CSE (Fig. 3B). Treatment with PAG caused a dose-dependent decrease in the rate of HCEC proliferation when compared to vehicle (PBS)-treated control cultures (Fig. 3A). Similarly, transfection of HCEC with a CSE-targeting siRNA significantly slowed down cell proliferation by 72 h compared to cells transfected with a non-targeting (NT) control siRNA (Fig. 3B).

CSE activity promotes both basal and cytokine stimulated HCEC migration. Tumor necrosis factor- α (TNF- α) and interleukin (IL)-10 play important physiological roles in restoring mucosal integrity following injury, in part, by stimulating epithelium restitution; a two-step process involving the breakdown of inter-epithelial cell-to-cell junctional complexes and induction of a migratory phenotype to facilitate wound closure [40–42]. Using transwell migration assays, we first assessed whether CSE activity and/or expression was required for basal chemotactic migration toward NIH3T3 fibroblast-conditioned culture medium. Pretreating the cells either with 1.5 mM or 3.0 mM PAG reduced HCEC migration toward the conditioned medium by an average of 41%, compared to PBS (vehicle)-treated control cultures (Fig. 4A). Similarly, transfecting HCECs with CSE-targeting siRNA sequences

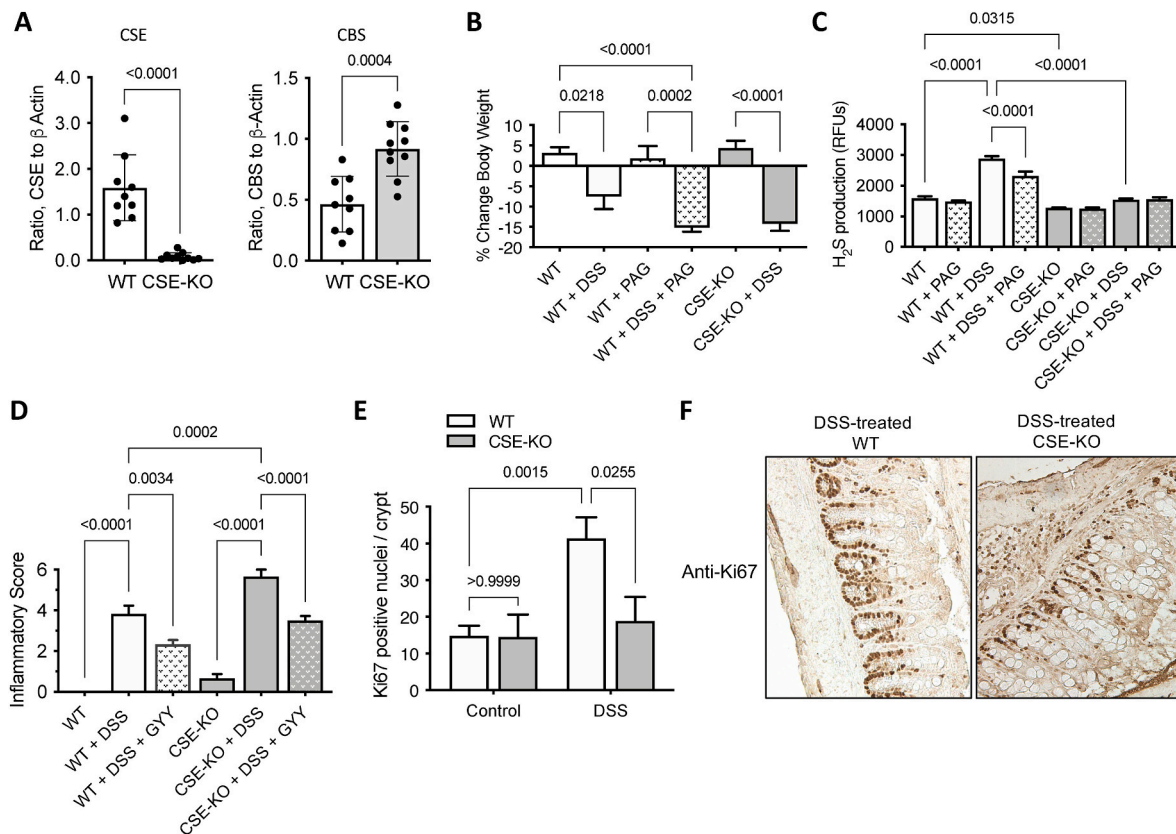


Fig. 2. Loss of CSE expression exacerbates acute inflammation and reduces epithelial proliferation. **A**) Densitometric analyses of western blots comparing CSE and CBS protein levels in colonic mucosa scrapings from CSE-KO (n = 9) and WT (n = 9) mice. (D'Agostino & Pearson Normality test, Unpaired *t*-test, two-tailed, bars represent mean \pm SD, *p* values shown). **B**) Effects of dextran sulfate sodium salt (DSS) exposure (7 days) and DL-progargylglycine (PAG) treatment on mouse body weight, and **C**) colonic mucosa H_2S production. **D**) Effects of DSS and the exogenous H_2S donor GYY4137 (GYG) on colon inflammation. Statistical analyses of data in panels **B-D**: Shapiro-Wilk Normality test, one-way ANOVA, Tukey multiple comparisons, *p* values shown. **E**) Quantification of Ki67-positive cell nuclei per colonic crypt from WT and CSE-KO mice following exposure to DSS drinking water for 7 days (Two-way ANOVA, Tukey multiple comparisons). **F**) Representative images of colon tissue sections from DSS-treated WT and DSS-treated CSE-KO mice immunostained for the proliferation antigen Ki67 (brown) (200 \times magnification). (For interpretation of the references to color in this figure legend, the reader is referred to the Web version of this article.)

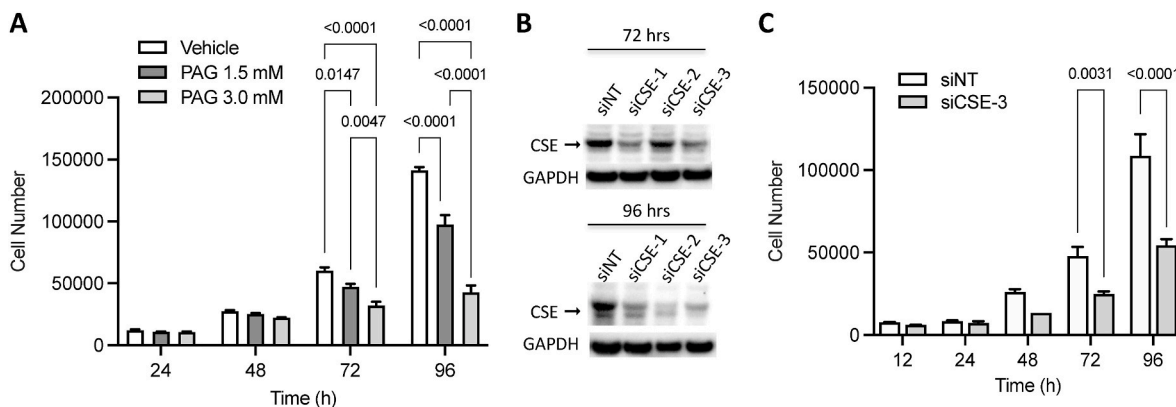


Fig. 3. CSE regulates the proliferation of human colonic epithelial cells in culture. **A**) Dose-dependent inhibitory effects of PAG on Human Colon Epithelial Cell (HCEC) proliferation. **B**) Western blot showing effects of CSE-targeting siRNAs on protein expression at 72 and 96 h post siRNA transfection. **C**) Effect of siRNA-mediated downregulation of CSE on HCEC proliferation (siCSE-3 sense: 5'-CUAUGUAUUCUGCAACAAATT-3'; antisense: 5'-UUUGUUGCAGAAUACAUGAA-3', Ambion Life Technologies, ThermoFisher Scientific, USA). Statistical analyses of data in panels **A** and **B**: Two-way ANOVA, Sidák's multiple comparisons, *p* values shown.

significantly inhibited migration, compared to cells transfected with a NT siRNA (Fig. 4B).

Next, to determine whether TNF- α and IL-10 regulate HCEC migration in a CSE-dependent manner, cell cultures were first pretreated either with PBS (vehicle control) or PAG (3 mM) for 1 h, then

disassociated and seeded into the top chambers of transwells with or without TNF- α (10 ng/ml) or IL-10 (1 ng/ml) and incubated for an additional 12 h. The bottom chamber of the transwell contained NIH3T3 fibroblast-conditioned medium with or without the same concentrations of cytokine. TNF- α stimulated a 1.6-fold increase in HCEC migration

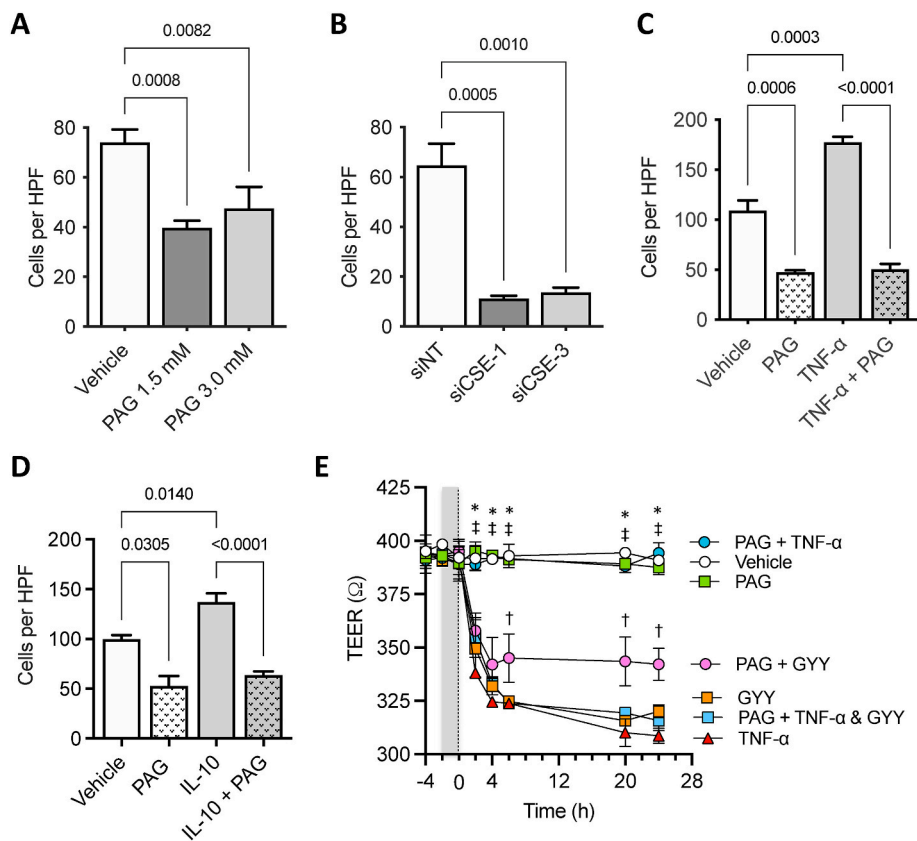


Fig. 4. CSE regulates cellular processes involved in epithelium restitution. A) Effect of PAG-mediated CSE inhibition on basal HCEC migration. B) Effects of siRNA-mediated downregulation of CSE expression on basal HCEC migration (siCSE-1 sense: 5'-GCAUCUGAAUUUGGAUUA-3'; anti-sense: 5'-UUAUCCAAAUCAGAUUC-3', Ambion Life Technologies, ThermoFisher Scientific, USA). C) Effects of PAG-mediated CSE inhibition on basal and TNF- α -stimulated (10 ng/ml) HCEC migration. D) Effects of PAG-mediated CSE inhibition on basal and IL-10-stimulated (10 ng/ml) HCEC migration. Statistical analyses of data in panel A–D: Shapiro-Wilk Normality test, one-way ANOVA, Tukey multiple comparisons, p values shown). E) Effects of PAG (3 mM) on GYY (0.4 mM) and TNF- α (1 ng/ml) regulation of TEER. Gray band between time –2 and 0 h indicates the time-period of PAG pretreatment. TNF- α and/or GYY was added to cultures at time = 0 (dotted-line). Statistical analysis of data in panel E: 2-way ANOVA, Tukey multiple comparison test, * $p < 0.0001$ [Vehicle vs. TNF- α or GYY], † $p < 0.01$ [PAG + GYY vs. GYY], ‡ $p < 0.0001$ [PAG or PAG + TNF- α vs. PAG vs. PAG + GYY or PAG + TNF- α & GYY].

toward fibroblast conditioned medium, compared to vehicle-treated control cultures (Fig. 4C). Pretreating cells with PAG inhibited both basal and TNF- α -stimulated HCEC migration (Fig. 4C). Similarly, IL-10 treatment also enhanced HCEC migration toward the fibroblast-conditioned medium, an effect that was blocked by pretreating the cells with PAG (Fig. 4D).

CSE activity is required for TNF- α regulation of transepithelial permeability. To assess the role of CSE in regulating inter-epithelial cell junctional complex permeability, monolayer cultures of HCECs were pretreated for 2 h with PAG or PBS (vehicle) and then stimulated with TNF- α (1 ng/ml and 10 ng/ml). Changes in transepithelial electrical resistance (TEER) were measured at 2-, 4-, 6-, 20-, and 24-h time-points (Fig. 4E). TNF- α (1 ng/ml) caused a significant decrease in TEER by 2 h, which persisted until the end of the experiment (Fig. 4E Vehicle vs. TNF- α ; * $p < 0.0001$). Pretreating the cultures with PAG (3 mM) had no effect on TEER when compared to PBS-treated control cultures. However, PAG completely blocked the TNF- α -induced increase in *trans*-epithelial permeability (Fig. 4E), suggesting that TNF- α regulation of inter-epithelial junctional complexes requires CSE activity (i.e., CSE-dependent H₂S production). Similar results were observed in cultured treated with 10 ng/ml TNF- α (data not shown). To test the effects of H₂S on TEER, we treated HCEC monolayer with GYY (0.4 mM) alone and in combination with TNF- α . When used alone, GYY mimicked the effects of TNF- α , causing a significant increase in transepithelial permeability by 2 h that persisted over the 24-h time course (Fig. 4E, Vehicle vs. GYY; * $p < 0.0001$). PAG pretreatment only partially inhibited the decrease in TEER induced by the H₂S donor (Fig. 4E, PAG + GYY vs. GYY, † $p < 0.01$). Importantly, when GYY was combined with TNF- α , it prevented the inhibitory effects of PAG on TNF- α -regulated TEER (Fig. 4E, PAG + TNF- α vs. PAG + TNF- α & GYY, ‡ $p < 0.0001$), supporting the hypothesis that CSE-produced H₂S mediates TNF- α regulation of transepithelial permeability in the colon. Together these studies validate, *in vitro*, that CSE activity and H₂S regulate key cellular processes involved in both

colonic epithelium restitution and proliferation; cellular processes were found to be critical to the normal repair and maintenance of mucosa integrity.

Loss of CSE activity accelerates the development of CAC. Having confirmed the importance of CSE activity in regulating colonic inflammation and injury repair response, we next assessed the effects of CSE gene deletion on the development and progression of CAC. CSE-KO and WT control animals were given a single injection of the mutagen azoxymethane [AOM (10 mg/kg)] on day zero and then divided into groups of 10 mice each to receive up to 3 cycles of DSS-induced colitis (Fig. 5A). Colons (from the ileocecal valve to the anus) were harvested at the end of each DSS cycle as well as on day 80 post-AOM injection (Fig. 5A). Each colon was cut longitudinally to reveal the mucosal surface and digitally imaged. Because day 21 tumors were microscopic, we first fixed the tissues and stained them with methylene blue. Small tumors and large aberrant crypt foci (ACF) were counted at 40 \times magnification. To quantify tumor burden on days 42, 63, and 80, the percentage of total tumor area was calculated by dividing the sum of the areas of all visible tumors by the total area of the colon using ImageJ software. An example of a digital image and analysis is shown in Fig. 5B. Compared to WT mice, CSE-KO mice had more small tumors/ACF on day 21 than WT mice (Fig. 5C) and significantly greater tumor burden at days 42 and 63 (Fig. 5D). However, by day 80 the tumor burdens of surviving WT and CSE KO mice were not significantly different (Fig. 5C; $p < 0.3232$), suggesting that the protective role of CSE is more pronounced at the early stage of CAC development.

CSE-KO mice exhibit reduced survival and more advanced disease. Loss of CSE expression had a significant negative impact on survival. We observed an approximately 25% increase in mortality of CSE-KO mice compared to WT animals between days 50 and 63 (Fig. 6A, * $p < 0.05$, Log-rank (Mantel-Cox) test]. The loss of mice in the CSE-KO group during this time interval may also be a reason why we did not observe a significant difference in tumor burden between these groups at Day 80.

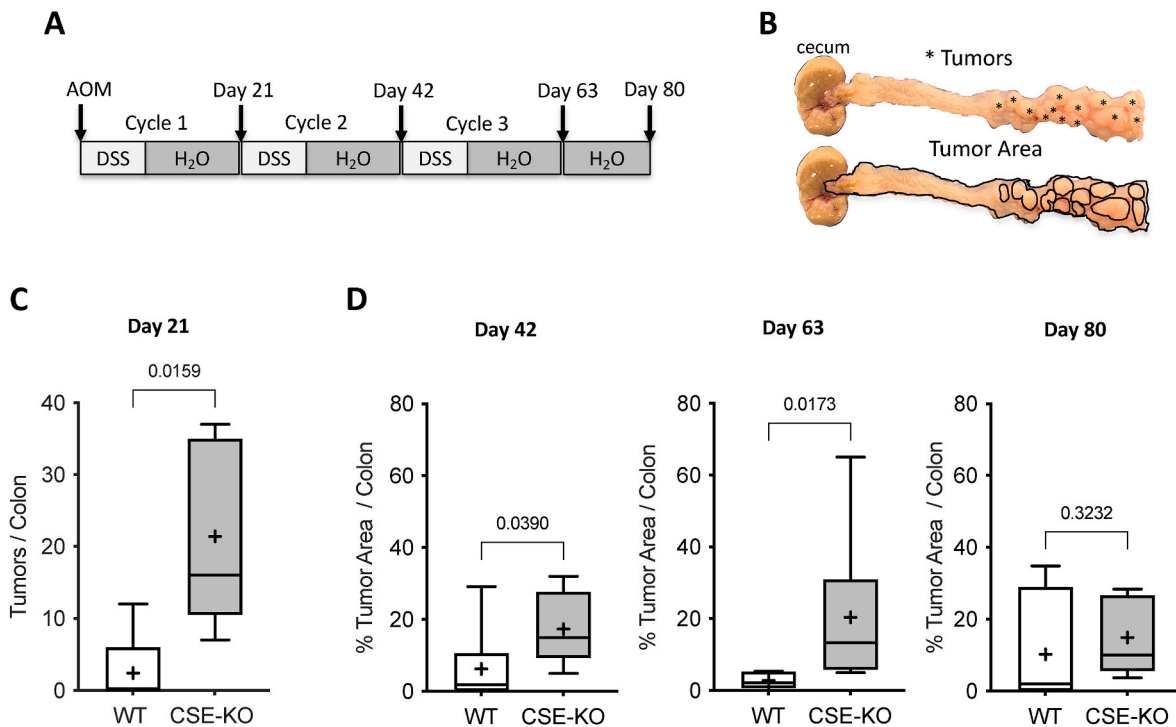


Fig. 5. Loss of CSE accelerates the development of CAC in AOM/DSS-treated mice. A) Timeline of the AOM/DSS colitis-associated carcinogenesis experiment. Mice received up to three exposures (cycles) of drinking water containing DSS. Arrows indicate when mice received an injection of the mutagen azoxymethane (AOM) and the days when colon tissue was harvested to assess tumor burden. B) Example images of a CSE-KO colon harvested on day 63. Asterisks on the top image indicate individual tumors. The percentage of tumor burden (area) was calculated by dividing the sum of the areas of all the individual tumors (outlined in black in the bottom image) by the area of the total colon (also outlined in black) using Image J software. C&D) Box and Whisker plots comparing the effects of AOM and DSS treatment of WT and CSE-KO mice on tumor number at Day 21 C) and tumor burden (i.e., % Tumor Area/Colon) at Days 42, 63, and 80 D) (Mann-Whitney test, two-tailed, exact p values shown, +: mean).

Necropsies revealed that most deaths of CSE-KO mice, between days 50 and 63, were due to tumor-associated bowel obstruction. In contrast, all deaths (~10%) of WT mice and the early deaths (≤ 20 days) of CSE-KO mice were due to complications from colitis, not tumor burden.

Histological evaluations of tumors from both WT and CSE-KO colons revealed a spectrum of pathological abnormalities, including epithelial hyperplasia, low-grade adenomatous polyps, high-grade adenomas, and invasive carcinoma (Fig. 6B). A comparison of the relative frequencies of

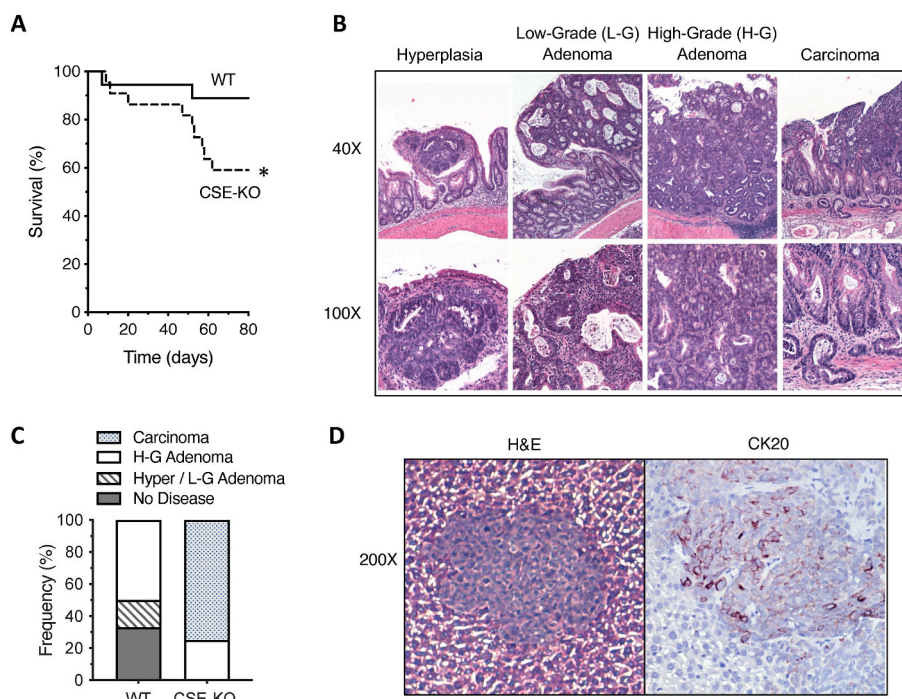


Fig. 6. CSE-KO mice treated with AOM and DSS exhibit reduced survival and more severe CAC than WT mice. A) Effect of AOM/DSS treatment on WT and CSE-KO mouse survival [Log-rank (Mantel-Cox) test, *p = 0.0284] (n = 10 per group X 3 experimental repeats). B) Hematoxylin and Eosin (H&E) stained mouse colon tissue, prepared using the Swiss roll technique, showing examples of the different histological categories of tumors observed in AOM/DSS treated mice at Day 80 (Top row: 40 \times magnification, Bottom row: 100 \times). C) A comparison of the relative frequencies of each category of lesion observed in the colons of AOM/DSS-treated WT and CSE-KO mice. Data are expressed as the percentage of colons within each group with a specific type of lesion (n = 6 surviving mice per group X 3 experimental repeats). D) Example of a metastatic colon tumor in the liver of an AOM/DSS-treated CSE-KO mouse (200 \times magnification). H&E-stained image of the liver metastasis (left) and an adjacent serial cut section (right) with immunohistochemical staining for the colon cancer cell marker Cytokeratin 20 [CK20 (red-brown color), Hematoxylin (blue color)]. (For interpretation of the references to color in this figure legend, the reader is referred to the Web version of this article.)

each type of lesion in the colons of WT and CSE-KO mice at day 80 revealed that CSE-KO mice exhibited a more advanced disease (Fig. 6C). All surviving CSE-KO mice had tumors, with 75% exhibiting invasive adenocarcinoma (Fig. 6C), including one mouse that also developed liver metastasis (Fig. 6D). Immunostaining of liver sections with the colon cancer cell marker Cytokeratin 20 (CK20) confirmed that the liver lesions were colon cancer metastases (Fig. 6D). By comparison, 30% of the colons from AOM/DSS-treated WT mice showed no tumors at day 80, 20% exhibited only hyperplastic polyps or low-grade adenomas, and 50% of the WT colons contained high-grade adenomatous polyps (Fig. 6C). None of the AOM/DSS-treated WT mice developed invasive adenocarcinoma within the time-period of the experiment (Fig. 6C), demonstrating that CSE expression slows down CAC initiation and progression in this model.

Reestablishing CSE expression in the BM of CSE-KO mice suppresses the development of CAC. BM-derived cells play a crucial role in tissue repair, particularly in the context of chronic inflammation or severe injury [43–46]. To assess the role of CSE activity from BM-derived cells in the development of CAC, we produced 2 groups of chimeric animals by transplanting WT BM (i.e., CSE-expressing BM cells) into lethally irradiated CSE-KO mice and CSE-KO BM into irradiated WT mice. These mice were compared to two control groups that were isografts (i.e., transplantation of tissue between two genetically identical mice) of BM from donor WT mice transplanted into WT recipient mice, and CSE-KO BM transplanted into CSE-KO mice. The AOM/DSS model of CAC was initiated 4 weeks after BM transplantation (i.e., 2 weeks after ending antibiotic treatments to allow repopulation of the colonic microbiome). All mice received 1 injection of AOM (10 mg/kg) followed by 7 days of 2% DSS drinking water and an additional 14 days of normal water. On day 21, colons were harvested and stained with methylene blue to quantify ACF and small tumors. Additionally, mucosal scrapings were collected for RNA preparations and cytokine detection by

RT-qPCR. Our decision to harvest tissue after one cycle of AOM/DSS was based on our data showing a significant difference in tumor multiplicity between WT and CSE-KO mice at day 21 (Fig. 5C) and by recent reports in the literature showing that the BM reacts quickly to mucosal injury (within 1 day). Furthermore, the transition from an inflammatory response to mucosa proliferation at the site of injury is completed in approximately 3 weeks [45,47]. Thus, this time frame allows the observation of CAC initiation (i.e., ACF formation) as well as early tumor progression (i.e., tumor growth). ACF and small tumors were counted in each methylene blue-stained colon at 200X and 40X magnification, respectively, by four different observers (M.M, E.J.H, F.A-A, S.D.) blinded to the identity of the specimens. Representative images of an ACF at 200X and tumor at 40X are shown (Fig. 7A).

Similarly, to data shown in Fig. 5, isografted CSE-KO mice developed significantly more ACF and tumors than isografted WT animals (Fig. 7B, CSE-KO (BM) to CSE-KO vs. WT (BM) to WT, $***p < 0.001$). On average, isografted CSE-KO mice developed 19.5 ACF (SD \pm 14.9) and 8.5 tumors (SD \pm 3.9) by Day 21, whereas WT mice developed only 6.5 ACF (SD \pm 3.6) and 2.2 small tumors (SD \pm 2.1) per colon over the same time period (Fig. 7B&C). Allografting CSE-KO animals with CSE-expressing BM cells from WT mice significantly reduced the numbers of both ACF and tumors. The chimeric CSE-KO mice exhibited less than half the number of ACF (8.8 ± 8.1 vs. 19.5 ± 14.9) and approximately one-third of the number of tumors (2.9 ± 2.6 vs. 8.5 ± 3.9) found in the isografted CSE-KO animals (Fig. 7B&C). The average numbers of ACF and tumors observed in the chimeric CSE-KO mice were not significantly different from the numbers observed in the isografted WT group (Fig. 7B&C, WT (BM) to CSE-KO vs. WT (BM) to WT, $p = 0.76$ and $p > 0.99$, respectively), demonstrating the suppressive function of CSE-expressing BM cells on the development of CAC. This conclusion was supported by the observation that WT mice transplanted with CSE-KO BM showed a significant increase in the number of ACF (Fig. 7B, $p < 0.05$). However, we

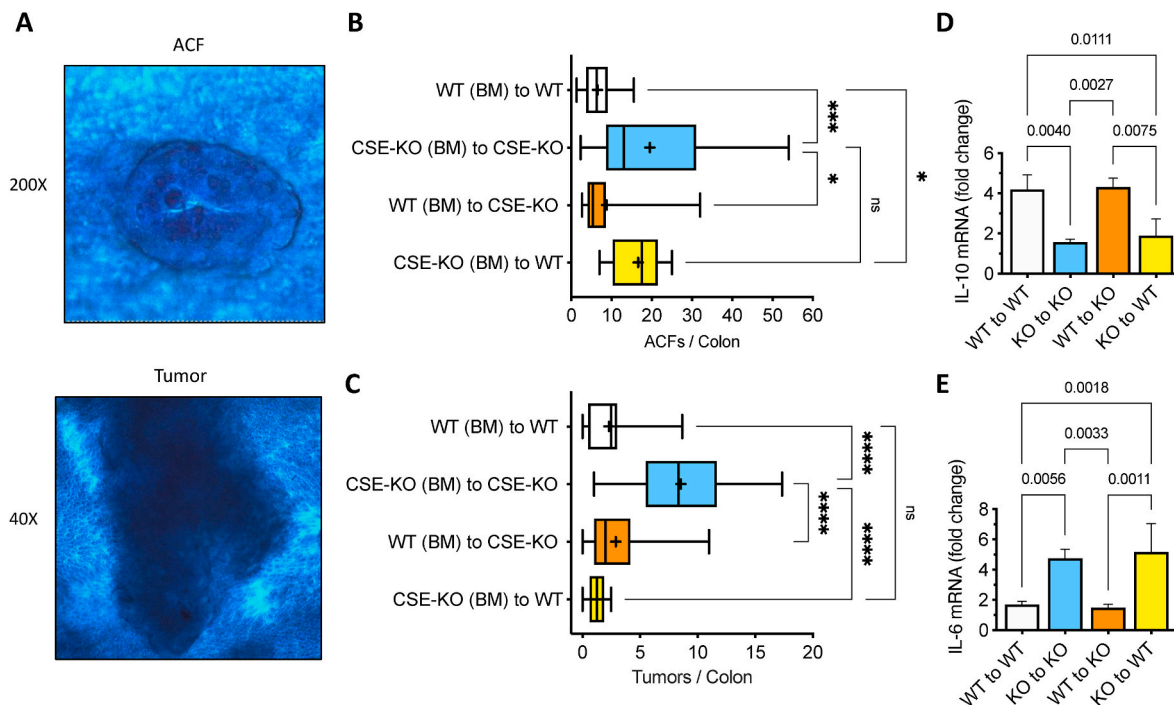


Fig. 7. CSE-expressing bone marrow cells suppress CAC development in CSE-KO mice. **A)** Example images of a single methylene-blue stained aberrant crypt focus (ACF) at 200 \times magnification and a small tumor at 40X. **B)** Box and Whisker plot comparing the effects of reciprocal bone marrow (BM) transplants on AOM/DSS-induced Aberrant Crypt Foci (ACF) formation (D'Agostino & Pearson Normality test, Brown-Forsythe and Welch ANOVA, $*p < 0.05$, $***p < 0.001$, + : mean). **C)** Box and Whisker plot comparing the effects of reciprocal bone marrow (BM) transplants on AOM/DSS-induced tumor formation (Kruskal-Wallis test, Dunn's multiple comparisons test, $****p < 0.0001$, +: mean). Effects of BM transplant on recipient mouse colonic mucosa IL-10 (**D**) and IL-6 (**E**) mRNA expression (Shapiro-Wilk Normality test, one-way ANOVA, Tukey's multiple comparison test, p values shown). (For interpretation of the references to color in this figure legend, the reader is referred to the Web version of this article.)

were surprised to see that despite the increase in ACF, the numbers of small tumors in the chimeric WT mice were not statistically different from the numbers seen in the WT isograft animals (Fig. 7C, $p > 0.99$), indicating that tumor progression (i.e., growth) was inhibited, despite that increase in neoplastic transformation.

CSE-expressing BM cells regulate the mucosal expression of IL-10 and IL-6 in AOM/DSS-treated mice. The cytokines IL-10 and IL-6 are key mediators linking inflammation to carcinogenesis. Generally, IL-10 functions to suppress inflammation and thus inhibits the development of CAC [48], whereas IL-6 enhances colitis and promotes both initiation and progression of colon cancer [49–51]. Additionally, H₂S has been shown to exert its anti-inflammatory effects, in part, by increasing IL-10 expression and downregulating IL-6 in various models of acute tissue injury and inflammation [52–54].

To assess the effects of CSE-expressing BM cells on colonic IL-10 and IL-6 mRNA expression, total RNA was isolated from the mucosal scrapings of AOM/DSS-treated mice. Quantitative RT-PCR assays revealed that IL-10 mRNA levels were significantly higher in the mucosa of isografted WT mice than isografted CSE-KO animals (Fig. 7D, WT to WT vs. KO to KO, $p = 0.004$). The opposite was seen for IL-6 mRNA; AOM/DSS treated isografted WT mice exhibited significantly lower levels of IL-6 message at the time of tissue harvest compared to isografted CSE-KO animals (Fig. 7E, WT to WT vs. KO to KO, $p = 0.0056$). Reestablishing CSE-expressing cells in the BM of chimeric CSE-KO mice increased mucosal expression of IL-10 (Fig. 7D, WT to KO vs. KO to KO, $p = 0.0027$) and suppressed levels of IL-6 mRNA (Fig. 7E, WT to KO vs. KO to KO, $p = 0.0033$). In contrast, the levels of IL-10 and IL-6 mRNA expression in AOM/DSS-treated chimeric WT mice were like those observed in the mucosa of isografted CSE-KO mice, with relatively low levels of IL-10 mRNA (Fig. 7D, WT to KO vs. KO to KO) and elevated levels of IL-6 (Fig. 7E, WT to KO vs. KO to KO). Together these data demonstrate that CSE-expressing BM cells are required to increase the mucosal expression of IL-10 mRNA and suppress colonic IL-6 levels in AOM/DSS-treated mice.

4. Discussion

This study was motivated by a growing body of experimental and clinical data suggesting that downregulation of TSP activity may play a role in the pathogenesis of CAC, a subtype of colorectal cancer (CRC) that is most frequently observed in patients with an extended history of unresolved IBD, particularly UC [55]. The data presented herein demonstrate that: 1) the TSP enzyme CSE is reduced in colonic biopsies from patients with UC, 2) loss of CSE expression exacerbates DSS-induced colitis in mice, 3) CSE stimulates normal human colon epithelial cell migration, proliferation, and transepithelial permeability, 4) CSE inhibits mucosal expression of IL-6 and stimulates IL-10 expression, and 5) loss of CSE in bone marrow-derived cells accelerates development and progression of colon cancer in the AOM/DSS mouse model of CAC.

Clinical studies have identified a significant positive association between hyperhomocysteinemia, IBD and colon cancer [24–31]. Homocysteine is a non-protein-forming sulfur amino acid that is generated by the demethylation of methionine. It is metabolized by either the TSP enzymes to produce cysteine or methylene tetrahydrofolate reductase (MTHFR), a key enzyme in the methionine remethylation pathway [56]. An elevated level of plasma homocysteine can be caused by mutations in these enzymes that play a key role in regulating circulating homocysteine levels. Mutations in MTHFR have only been identified in a subset of IBD patients suggesting that decreased TSP activity may also be involved in IBD associated hyperhomocysteinemia. Recently, Chen and colleagues reported downregulation of the TSP enzyme CBS in colon specimens from UC patients compared to healthy control samples [29]. In our assessment comparing a similar number of UC biopsy specimens and normal controls, CBS protein levels trended lower in UC, but the difference did not reach significance. However, we clearly demonstrated

that CSE is significantly downregulated in UC.

It is widely accepted that chronic inflammation of the gastrointestinal tract results in impaired physiological processes regulating immune homeostasis and tissue repair [57]. Our data generated with human colonic epithelial cells suggest that CSE plays a critical role in epithelial repair and regeneration and thus, its loss and/or decreased activity likely contributes to the pathogenesis of UC. Previously the importance of CBS in the maintenance of the epithelial barrier, and in the response to IBD relevant injury has been reported in cultured colon cancer cells [29]. Using the non-malignant, normal karyotype HCEC line, we demonstrated that CSE regulates colon epithelial cell proliferation, both basal and cytokine-stimulated epithelial cell migration and transepithelial permeability.

Using the AOM/DSS mouse model of CAC, we showed that loss of CSE expression accelerated the development of CAC and promoted disease progression, as indicated by the increased frequency of invasive carcinoma and metastasis in CSE-KO mice compared to WT animals. Additionally, reciprocal BM transplantation experiments established that CSE, specifically expressed by BM-derived cells, exerted a tumor suppressor function since WT BM cells (i.e., CSE-expressing BM cells) transplanted into CSE-KO mice were sufficient to dramatically reduce colitis-associated tumor formation. However, it remains to be determined which subset of BM-derived cells is most affected by the reduction of CSE in UC and subsequent initiation of CAC.

The BM functions as a reservoir of stem and progenitor cells, including mesenchymal stem cells, hematopoietic stem cells, and endothelial progenitor cells, limiting inflammation at the site of injury and initiating the cellular processes of proliferation, migration, and differentiation critical to restoring tissue integrity and homeostasis [44, 46]. A recent study using *Helicobacter hepaticus* induced colitis demonstrated that chronic oral administration of the H₂S donor DATS reduced colon inflammation by limiting the recruitment of granulocytic myeloid-derived suppressor cells [58]. Also, H₂S showed to promote the resolution of inflammation by inducing neutrophil apoptosis [59] and driving the differentiation of macrophages towards the anti-inflammatory “M2” phenotype [60]. In addition, our key finding that tumor growth was inhibited in the WT chimeric mice, could be partially explained by the lack of CSE-expressing endothelial progenitor cells (EPCs) from the CSE KO BM inhibiting tumor angiogenesis, a critical step in tumor development and progression. Supporting this interpretation, Lui and colleagues have shown that siRNA-mediated downregulation of CSE in BM-derived EPCs inhibited angiogenesis and wound healing in an animal model of type 2 diabetes [61]. Proof of this mechanism in the AOM/DSS model of CAC will require selectively downregulating CSE in BM-derived EPCs.

Our study also provides evidence that the lack of CSE in BM-derived cells affects the balance of IL-6 and IL-10 expression in the colonic mucosa. These cytokines are important physiological regulators of inflammation in the gastrointestinal tract, and their dysregulation results in chronic inflammation and cancer. Indeed, an increased level of the pro-inflammatory cytokine IL-6 has been detected in the serum and tissue biopsies of patients with UC and colon cancer, correlating with the severity of disease in UC and poor survival prognosis in colon cancer [62–64]. Also, elevated IL-6 and soluble IL-6 receptor levels have been documented in experimental animal models of colitis and CAC, where persistent IL-6 signaling has been shown to exacerbate inflammation and promote carcinogenesis and disease progression [65–68]. Conversely, genome-wide association studies have revealed strong links between mutations that reduce IL-10 expression and/or secretion and the development of IBD [69–73], while IL-10 receptor signaling promotes the resolution of mucosal inflammation by regulating immune homeostasis, which in turn inhibits inflammation-associated carcinogenesis [74,75].

Additionally, the function of CSE and CBS in UC and CAC are most likely not redundant since CSE-KO mice exhibit an upregulation of CBS expression, compared to WT animals (data not shown). However, the

increased CBS expression in CSE-KO mice was insufficient to increase mucosal H₂S-production in response to DSS-induced epithelium injury or reduce mucosa inflammation. Interestingly, the upregulation of CBS has been shown by us and others to be among the factors contributing to the development of sporadic CRC [76,77].

In 2013, our group was the first that reported the aberrant upregulation of CBS in human CRC specimens and colon cancer-derived cell lines and demonstrated that inhibition of CBS expression and/or activity had anti-tumor effects. Following this discovery, we found that CBS expression was increased in human adenomatous polyps and that experimental upregulation of CBS in a premalignant colonic epithelial cell line (NCM356) caused extensive metabolic reprogramming and induction of an invasive tumorigenic phenotype [38]. Therefore, based on these findings, we speculate that an enhanced CBS activity may contribute to driving colon carcinogenesis and tumor progression via metabolic alterations. It is also worth noting that the pathogenetic mechanisms underlying CAC development and sporadic CRC have significant similarities and major differences [6]. For instance, during CAC development, multiple areas of the colon are involved, whereas dysplasia in CRC is focal. CAC has been preceded by chronic inflammation of the colon for years, which phenomenon does not exist in sporadic CRC development. Regarding oncogenic gene mutations, there are remarkable similarities in sporadic CRC and CAC (e.g., KRAS activation) [78]. However, while loss of function mutations in the tumor suppressor gene APC is an early event driving carcinogenesis in sporadic CRC, it appears much later and less frequently in CAC [79]. In contrast, while loss of function mutations in p53 have been found to be the most dominant oncogenic driving force in CAC in over 80% of patients, it is much less significant in sporadic CRC with less than 50% prevalence [80]. Differences between the roles of CSE and CBS in CAC and CRC may stem from the distinct patterns of cancer-driving mutations occurring in the genomes of these cancer cells. Considering all the above-mentioned reports and several studies from other research groups detailing the role of CSE or CBS in colitis [19–23], we speculate that CSE has a major role in regulating and modulating inflammation and tumor initiation in the presence of chronic inflammation of the colon. Further studies are needed to define the functional differences between these TSP enzymes, CSE and CBS, with respect to the development and progression of CAC and sporadic CRC.

In conclusion, for the first time, we provide a comprehensive report suggesting a critical role of the key enzyme CSE in the TSP metabolic pathway as a possible new player in the protection against UC and CAC development. Our data demonstrate that reduced endogenous CSE level within both epithelial and BM-derived cells is likely to be involved in the development of CAC. Our data also suggest that compensating for the lack of CSE by an exogenous H₂S donor can be an attractive avenue for developing novel, non-invasive CAC prophylactic strategies, as well as assessing CSE expression and/or activity can be used to predict CAC risk in patients with UC.

Author contributions

Conceptualization: M.R. Hellmich, C. Chao, I.V. Pinchuk, K. Modis, Data Curation: K.K. Thanki, P. Johnson, C. Philips, E.J. Higgins, M. Maskey, R. Villéger, F. Arroyo-Almenas, E. Beswick, K. Modis, Formal Analysis: M.R. Hellmich, I.V. Pinchuk, E. Beswick, K. Modis, Funding Acquisition: M.R. Hellmich, I.V. Pinchuk, C. Szabo, K. Modis, Investigation: K.K. Thanki, P. Johnson, E.J. Higgins, M. Maskey, C. Philips, R. Villéger, S. Dash, F. Arroyo-Almenas, A. Abdollahi Govar, B. Tian, K. Modis, Methodology: R. Wang, Project Administration: M.R. Hellmich, Resources: R. Wang, I.V. Pinchuk, E. Beswick, Supervision: M.R. Hellmich, C. Chao, I.V. Pinchuk, K. Modis, Validation: M.R. Hellmich, C. Chao, I.V. Pinchuk, Visualization: K.K. Thanki, P. Johnson, E. Beswick, M.R. Hellmich, Writing-Original Draft Preparation: K.K. Thanki, P. Johnson, M.R. Hellmich, Writing-Review & Editing: M.R. Hellmich, C. Chao, I.V. Pinchuk, C. Szabo, K. Modis

Funding sources

Drs. Thanki and Johnson were supported by the T32 training grant from the National Institutes of Health/NIDDK (DK007639), Bethesda, USA. Drs. Hellmich and Szabo were or currently are funded by the Cancer Prevention & Research Institute of Texas (CPRIT), DP150074, Texas, USA, The National Institutes of Health/NCI (R01CA175803), Bethesda, USA, and the Swiss Krebsliga (KLS-4504-08-2018). Dr. Modis is currently funded by the Department of Defense, Career Development Award (W81XWH2010641) and the American Cancer Society, Research Scholar Grant (RSG-21-027-01-CSM).

Declaration of competing interest

The authors declare no conflicts of interest.

Acknowledgements

KM would like to thank Melanie E. Connolly for the graphical abstract illustration.

References

- [1] J.A. Eaden, K.R. Abrams, J.F. Mayberry, The risk of colorectal cancer in ulcerative colitis: a meta-analysis, *Gut* 48 (4) (2001) 526–535.
- [2] J.E. Baars, E.J. Kuipers, M. van Haastert, J.J. Nicolai, A.C. Poen, C.J. van der Woude, Age at diagnosis of inflammatory bowel disease influences early development of colorectal cancer in inflammatory bowel disease patients: a nationwide, long-term survey, *J. Gastroenterol.* 47 (12) (2012) 1308–1322.
- [3] T. Jess, C. Rungoe, L. Peyrin-Biroulet, Risk of colorectal cancer in patients with ulcerative colitis: a meta-analysis of population-based cohort studies, *Clin. Gastroenterol. Hepatol.* 10 (6) (2012) 639–645.
- [4] M.W. Lutgens, F.P. Vlegaar, M.E. Schipper, P.C. Stokkers, C.J. van der Woude, D. W. Hommes, D.J. de Jong, G. Dijkstra, A.A. van Bodegraven, B. Oldenburg, M. Samsom, High frequency of early colorectal cancer in inflammatory bowel disease, *Gut* 57 (9) (2008) 1246–1251.
- [5] L.A. Feagins, R.F. Souza, S.J. Spechler, Carcinogenesis in IBD: potential targets for the prevention of colorectal cancer, *Nat. Rev. Gastroenterol. Hepatol.* 6 (5) (2009) 297–305.
- [6] D.C. Rubin, A. Shaker, M.S. Levin, Chronic intestinal inflammation: inflammatory bowel disease and colitis-associated colon cancer, *Front. Immunol.* 3 (2012) 107.
- [7] M. Yashiro, Ulcerative colitis-associated colorectal cancer, *World J. Gastroenterol.* 20 (44) (2014) 16389–16397.
- [8] S. Danese, A. Mantovani, Inflammatory bowel disease and intestinal cancer: a paradigm of the Yin-Yang interplay between inflammation and cancer, *Oncogene* 29 (23) (2010) 3313–3323.
- [9] N. Dilek, A. Papapetropoulos, T. Toliver-Kinsky, C. Szabo, Hydrogen sulfide: an endogenous regulator of the immune system, *Pharmacol. Res.* 161 (2020), 105119.
- [10] B. Gemic, J.L. Wallace, Anti-inflammatory and cytoprotective properties of hydrogen sulfide, *Methods Enzymol.* 555 (2015) 169–193.
- [11] D.R. Linden, Hydrogen sulfide signaling in the gastrointestinal tract, *Antioxidants Redox Signal.* 20 (5) (2014) 818–830.
- [12] S.B. Singh, H.C. Lin, Hydrogen sulfide in physiology and diseases of the digestive tract, *Microorganisms* 3 (4) (2015) 866–889.
- [13] J.L. Wallace, M. Dickey, W. McKnight, G.R. Martin, Hydrogen sulfide enhances ulcer healing in rats, *Faseb. J.* 21 (14) (2007) 4070–4076.
- [14] J.L. Wallace, J.G. Ferraz, M.N. Muscara, Hydrogen sulfide: an endogenous mediator of resolution of inflammation and injury, *Antioxidants Redox Signal.* 17 (1) (2012) 58–67.
- [15] J.L. Wallace, A. Ianaro, G. de Nucci, Gaseous mediators in gastrointestinal mucosal Defense and injury, *Dig. Dis. Sci.* 62 (9) (2017) 2223–2230.
- [16] J.L. Wallace, R.W. Blackler, M.V. Chan, G.J. Da Silva, W. Elsheikh, K.L. Flannigan, I. Gamaniek, A. Manko, L. Wang, J.P. Motta, A.G. Buret, Anti-inflammatory and cytoprotective actions of hydrogen sulfide: translation to therapeutics, *Antioxidants Redox Signal.* 22 (5) (2015) 398–410.
- [17] J.B. Kohl, A.T. Mellis, G. Schwarz, Homeostatic impact of sulfite and hydrogen sulfide on cysteine catabolism, *Br. J. Pharmacol.* 176 (4) (2019) 554–570.
- [18] Q. Yang, G.W. He, Imbalance of homocysteine and H₂S: significance, mechanisms, and therapeutic promise in vascular injury, *Oxid. Med. Cell. Longev.* 2019 (2019), 7629673.
- [19] K.L. Flannigan, T.A. Agbor, R.W. Blackler, J.J. Kim, W.I. Khan, E.F. Verdu, J. G. Ferraz, J.L. Wallace, Impaired hydrogen sulfide synthesis and IL-10 signaling underlie hyperhomocysteinemia-associated exacerbation of colitis, *Proc. Natl. Acad. Sci. U. S. A.* 111 (37) (2014) 13559–13564.
- [20] K.L. Flannigan, J.G. Ferraz, R. Wang, J.L. Wallace, Enhanced synthesis and diminished degradation of hydrogen sulfide in experimental colitis: a site-specific, pro-resolution mechanism, *PLoS One* 8 (8) (2013), e71962.
- [21] I. Hirata, Y. Naito, T. Takagi, K. Mizushima, T. Suzuki, T. Omatsu, O. Handa, H. Ichikawa, H. Ueda, T. Yoshikawa, Endogenous hydrogen sulfide is an anti-

- inflammatory molecule in dextran sodium sulfate-induced colitis in mice, *Dig. Dis. Sci.* 56 (5) (2011) 1379–1386.
- [22] J.P. Motta, K.L. Flannigan, T.A. Agbor, J.K. Beatty, R.W. Blackler, M.L. Workentine, G.J. Da Silva, R. Wang, A.G. Buret, J.L. Wallace, Hydrogen sulfide protects from colitis and restores intestinal microbiota biofilm and mucus production, *Inflamm. Bowel Dis.* 21 (5) (2015) 1006–1017.
- [23] J.L. Wallace, L. Vong, W. McKnight, M. Dickey, G.R. Martin, Endogenous and exogenous hydrogen sulfide promotes resolution of colitis in rats, *Gastroenterology* 137 (2) (2009) 569–578, 78 e1.
- [24] S. Akbulut, E. Altıparmak, F. Topal, E. Ozaslan, M. Kucukazman, O. Yonem, Increased levels of homocysteine in patients with ulcerative colitis, *World J. Gastroenterol.* 16 (19) (2010) 2411–2416.
- [25] A. Oussalah, J.L. Gueant, L. Peyrin-Biroulet, Meta-analysis: hyperhomocysteinemia in inflammatory bowel diseases, *Aliment. Pharmacol. Ther.* 34 (10) (2011) 1173–1184.
- [26] A. Papa, V. De Stefano, S. Danese, P. Chiusolo, S. Persichilli, I. Casorelli, B. Zappacosta, B. Giardina, A. Gasbarrini, G. Leone, G. Gasbarrini, Hyperhomocysteinemia and prevalence of polymorphisms of homocysteine metabolism-related enzymes in patients with inflammatory bowel disease, *Am. J. Gastroenterol.* 96 (9) (2001) 2677–2682.
- [27] P. Zezos, G. Papaioannou, N. Nikolaidis, T. Vasiliadis, O. Gioulema, N. Evgenidis, Hyperhomocysteinemia in ulcerative colitis is related to folate levels, *World J. Gastroenterol.* 11 (38) (2005) 6038–6042.
- [28] S. Zheng, W. Yang, C. Wu, L. Sun, D. Lin, X. Lin, L. Jiang, R. Ding, Y. Jiang, Association of ulcerative colitis with transcobalamin II gene polymorphisms and serum homocysteine, vitamin B12, and folate levels in Chinese patients, *Immunogenetics* 69 (7) (2017) 421–428.
- [29] S. Chen, S. Zuo, J. Zhu, T. Yue, D. Bu, X. Wang, P. Wang, Y. Pan, Y. Liu, Decreased expression of cystathionine beta-synthase exacerbates intestinal barrier injury in ulcerative colitis, *J. Crohns Colitis* 13 (8) (2019) 1067–1080.
- [30] J.M. Phelep, V. Ducros, J.L. Faucheron, B. Flourie, X. Roblin, Association of hyperhomocysteinemia and folate deficiency with colon tumors in patients with inflammatory bowel disease, *Inflamm. Bowel Dis.* 14 (2) (2008) 242–248.
- [31] A.H. Keshteli, V.E. Baracos, K.L. Madsen, Hyperhomocysteinemia as a potential contributor of colorectal cancer development in inflammatory bowel diseases: a review, *World J. Gastroenterol.* 21 (4) (2015) 1081–1090.
- [32] G. Yang, L. Wu, B. Jiang, W. Yang, J. Qi, K. Cao, Q. Meng, A.K. Mustafa, W. Mu, S. Zhang, S.H. Snyder, R. Wang, H2S as a physiologic vasorelaxant: hypertension in mice with deletion of cystathionine gamma-lyase, *Science* 322 (5901) (2008) 587–590.
- [33] A.I. Roig, U. Eskioçak, S.K. Hight, S.B. Kim, O. Delgado, R.F. Souza, S.J. Spechler, W.E. Wright, J.W. Shay, Immortalized epithelial cells derived from human colon biopsies express stem cell markers and differentiate in vitro, *Gastroenterology* 138 (3) (2010), 1012–10121 e1–5.
- [34] B. Chassaing, J.D. Aitken, M. Malleshappa, M. Vijay-Kumar, Dextran sulfate sodium (DSS)-induced colitis in mice, *Curr. Protoc. Im.* 104 (2014) 15 25 1–15 25 14.
- [35] C.A. Schneider, W.S. Rasband, K.W. Eliceiri, NIH Image to ImageJ: 25 years of image analysis, *Nat. Methods* 9 (7) (2012) 671–675.
- [36] A.B. Bialkowska, A.M. Ghaleb, M.O. Nandan, V.W. Yang, Improved Swiss-rolling technique for intestinal tissue preparation for immunohistochemical and immunofluorescent analyses, *JoVE* 113 (2016).
- [37] K. Geboes, R. Riddell, A. Ost, B. Jensfelt, T. Persson, R. Lofberg, A reproducible grading scale for histological assessment of inflammation in ulcerative colitis, *Gut* 47 (3) (2000) 404–409.
- [38] C.M. Phillips, J.R. Zatarain, M.E. Nicholls, C. Porter, S.G. Widen, K. Thanki, P. Johnson, M.U. Jawad, M.P. Moyer, J.W. Randall, J.L. Hellmich, M. Maskey, S. Qiu, T.G. Wood, N. Druzhyina, B. Szczesny, K. Modis, C. Szabo, C. Chao, M. R. Hellmich, Upregulation of cystathionine-beta-synthase in colonic epithelia reprograms metabolism and promotes carcinogenesis, *Cancer Res.* 77 (21) (2017) 5741–5754.
- [39] J. Zhu, M. Berisa, S. Schworer, W. Qin, J.R. Cross, C.B. Thompson, Transsulfuration activity can support cell growth upon extracellular cysteine limitation, *Cell Metabol.* 30 (5) (2019) 865–876 e5.
- [40] R. Al-Sadi, S. Guo, D. Ye, T.Y. Ma, TNF-alpha modulation of intestinal epithelial tight junction barrier is regulated by ERK1/2 activation of Elk-1, *Am. J. Pathol.* 183 (6) (2013) 1871–1884.
- [41] T.Y. Ma, M.A. Boivin, D. Ye, A. Pedram, H.M. Said, Mechanism of TNF-(alpha) modulation of Caco-2 intestinal epithelial tight junction barrier: role of myosin light-chain kinase protein expression, *Am. J. Physiol. Gastrointest. Liver Physiol.* 288 (3) (2005) G422–G430.
- [42] A.M. Marchiando, L. Shen, W.V. Graham, K.L. Edelblum, C.A. Duckworth, Y. Guan, M.H. Montrose, J.R. Turner, A.J. Watson, The epithelial barrier is maintained in vivo tight junction expansion during pathologic intestinal epithelial shedding, *Gastroenterology* 140 (4) (2011), 1208–12018 e1–2.
- [43] M. Quiros, H. Nishio, P.A. Neumann, D. Siuda, J.C. Brazil, V. Azcutia, R. Hilgarth, M.N. O'Leary, V. Garcia-Hernandez, G. Leoni, M. Feng, G. Bernal, H. Williams, P. H. Dedhia, C. Gerner-Smidt, J. Spence, C.A. Parkos, T.L. Denning, A. Nusrat, Macrophage-derived IL-10 mediates mucosal repair by epithelial WISP-1 signaling, *J. Clin. Invest.* 127 (9) (2017) 3510–3520.
- [44] R.C. Rennett, M. Sorkin, R.K. Garg, G.C. Gurtner, Stem cell recruitment after injury: lessons for regenerative medicine, *Regen. Med.* 7 (6) (2012) 833–850.
- [45] S. Shah, J. Ulm, Z.C. Sifri, A.M. Mohr, D.H. Livingston, Mobilization of bone marrow cells to the site of injury is necessary for wound healing, *J. Trauma* 67 (2) (2009) 315–321. ; discussion 21–2.
- [46] T.A. Wynn, K.M. Vannella, Macrophages in tissue repair, regeneration, and fibrosis, *Immunity* 44 (3) (2016) 450–462.
- [47] N.X. Landen, D. Li, M. Stahle, Transition from inflammation to proliferation: a critical step during wound healing, *Cell. Mol. Life Sci.* 73 (20) (2016) 3861–3885.
- [48] H.X. Wei, B. Wang, B. Li, IL-10 and IL-22 in mucosal immunity: driving protection and pathology, *Front. Immunol.* 11 (2020) 1315.
- [49] R. Atreya, M.F. Neurath, Involvement of IL-6 in the pathogenesis of inflammatory bowel disease and colon cancer, *Clin. Rev. Allergy Immunol.* 28 (3) (2005) 187–196.
- [50] K. Taniguchi, M. Karin, IL-6 and related cytokines as the critical lynchpins between inflammation and cancer, *Semin. Immunol.* 26 (1) (2014) 54–74.
- [51] M.J. Waldner, S. Foersch, M.F. Neurath, Interleukin-6—a key regulator of colorectal cancer development, *Int. J. Biol. Sci.* 8 (9) (2012) 1248–1253.
- [52] A.A. Fouad, H.M. Hafez, A. Hamouda, Hydrogen sulfide modulates IL-6/STAT3 pathway and inhibits oxidative stress, inflammation, and apoptosis in rat model of methotrexate hepatotoxicity, *Hum. Exp. Toxicol.* 39 (1) (2020) 77–85.
- [53] T. Li, B. Zhao, C. Wang, H. Wang, Z. Liu, W. Li, H. Jin, C. Tang, J. Du, Regulatory effects of hydrogen sulfide on IL-6, IL-8 and IL-10 levels in the plasma and pulmonary tissue of rats with acute lung injury, *Exp. Biol. Med.* 233 (9) (2008) 1081–1087.
- [54] J. Zeng, X. Lin, H. Fan, C. Li, Hydrogen sulfide attenuates the inflammatory response in a mouse burn injury model, *Mol. Med. Rep.* 8 (4) (2013) 1204–1208.
- [55] M. Scarpa, I. Castagliuolo, C. Castoro, A. Pozza, M. Scarpa, A. Kotsafti, I. Angriman, Inflammatory colonic carcinogenesis: a review on pathogenesis and immunosurveillance mechanisms in ulcerative colitis, *World J. Gastroenterol.* 20 (22) (2014) 6774–6785.
- [56] P. Durand, M. Prost, N. Loreau, S. Lussier-Cacan, D. Blache, Impaired homocysteine metabolism and atherothrombotic disease, *Lab. Invest.* 81 (5) (2001) 645–672.
- [57] H.S. de Souza, C. Fiocchi, Immunopathogenesis of IBD: current state of the art, *Nat. Rev. Gastroenterol. Hepatol.* 13 (1) (2016) 13–27.
- [58] P. De Cicco, T. Sanders, G. Cirino, K.J. Maloy, A. Ianaro, Hydrogen sulfide reduces myeloid-derived suppressor cell-mediated inflammatory response in a model of *Helicobacter hepaticus*-induced colitis, *Front. Immunol.* 9 (2018) 499.
- [59] M.A. Mariggio, V. Minunno, S. Riccardi, R. Santacroce, P. De Rinaldis, R. Fumarolo, Sulfide enhancement of PMN apoptosis, *Immunopharmacol. Immunotoxicol.* 20 (3) (1998) 399–408.
- [60] L. Miao, X. Xin, H. Xin, X. Shen, Y.Z. Zhu, Hydrogen sulfide recruits macrophage migration by integrin beta1-src-FAK/pyk2-rac pathway in myocardial infarction, *Sci. Rep.* 6 (2016), 22363.
- [61] F. Liu, D.D. Chen, X. Sun, H.H. Xie, H. Yuan, W. Jia, A.F. Chen, Hydrogen sulfide improves wound healing via restoration of endothelial progenitor cell functions and activation of angiotensin-1 in type 2 diabetes, *Diabetes* 63 (5) (2014) 1763–1778.
- [62] C. Belluco, D. Nitti, M. Frantz, P. Toppan, D. Basso, M. Plebani, M. Lise, J. M. Jessup, Interleukin-6 blood level is associated with circulating carcinoembryonic antigen and prognosis in patients with colorectal cancer, *Ann. Surg. Oncol.* 7 (2) (2000) 133–138.
- [63] R. Carey, I. Jurickova, E. Ballard, E. Bonkowski, X. Han, H. Xu, L.A. Denson, Activation of an IL-6:STAT3-dependent transcriptome in pediatric-onset inflammatory bowel disease, *Inflamm. Bowel Dis.* 14 (4) (2008) 446–457.
- [64] J. Zeng, Z.H. Tang, S. Liu, S.S. Guo, Clinicopathological significance of overexpression of interleukin-6 in colorectal cancer, *World J. Gastroenterol.* 23 (10) (2017) 1780–1786.
- [65] D.A. Braun, M. Fribourg, S.C. Sealfon, Cytokine response is determined by duration of receptor and signal transducers and activators of transcription 3 (STAT3) activation, *J. Biol. Chem.* 288 (5) (2013) 2986–2993.
- [66] S. Grivennikov, E. Karin, J. Terzić, D. Mucida, G.Y. Yu, S. Vallabhapurapu, J. Scheller, S. Rose-John, H. Cheroutre, L. Eckmann, M. Karin, IL-6 and Stat3 are required for survival of intestinal epithelial cells and development of colitis-associated cancer, *Cancer Cell* 15 (2) (2009) 103–113.
- [67] J. Han, Q. Xi, Q. Meng, J. Liu, Y. Zhang, Y. Han, Q. Zhuang, Y. Jiang, Q. Ding, G. Wu, Interleukin-6 promotes tumor progression in colitis-associated colorectal cancer through HIF-1 alpha regulation, *Oncol. Lett.* 12 (6) (2016) 4665–4670.
- [68] Y. Li, C. de Haar, M. Chen, J. Deuring, M.M. Gerrits, R. Smits, B. Xia, E.J. Kuipers, C.J. van der Woude, Disease-related expression of the IL6/STAT3/SOCS3 signalling pathway in ulcerative colitis and ulcerative colitis-related carcinogenesis, *Gut* 59 (2) (2010) 227–235.
- [69] A. Franke, T. Balschun, T.H. Karlsen, J. Sventoraityte, S. Nikolaus, G. Mayr, F. S. Domingues, M. Albrecht, M. Nothnagel, D. Ellinghaus, C. Sina, C.M. Onnie, R. K. Weersma, P.C. Stokkers, C. Wijmenga, M. Gazouli, D. Strachan, W.L. McArdle, S. Vermeire, P. Rutgeerts, P. Rosenstiel, M. Krawczak, M.H. Vatn, Is group, C. G. Mathew, S. Schreiber, Sequence variants in IL10, ARPC2 and multiple other loci contribute to ulcerative colitis susceptibility, *Nat. Genet.* 40 (11) (2008) 1319–1323.
- [70] C.J. Moran, T.D. Walters, C.H. Guo, S. Kugathasan, C. Klein, D. Turner, V. M. Wolters, R.H. Bandsma, M. Mouzaki, M. Zachos, J.C. Langer, E. Cutz, S. M. Benseler, C.M. Roifman, M.S. Silverberg, A.M. Griffiths, S.B. Snapper, A. M. Muise, IL-10R polymorphisms are associated with very-early-onset ulcerative colitis, *Inflamm. Bowel Dis.* 19 (1) (2013) 115–123.
- [71] E. Noguchi, Y. Homma, X. Kang, M.G. Netea, X. Ma, A Crohn's disease-associated NOD2 mutation suppresses transcription of human IL10 by inhibiting activity of the nuclear ribonucleoprotein hnRNP-A1, *Nat. Immunol.* 10 (5) (2009) 471–479.
- [72] A.I. Thompson, C.W. Lees, Genetics of ulcerative colitis, *Inflamm. Bowel Dis.* 17 (3) (2011) 831–848.

- [73] H. Zhu, X. Lei, Q. Liu, Y. Wang, Interleukin-10-1082A/G polymorphism and inflammatory bowel disease susceptibility: a meta-analysis based on 17,585 subjects, *Cytokine* 61 (1) (2013) 146–153.
- [74] K.L. Dennis, N.R. Blatner, F. Gounari, K. Khazaie, Current status of interleukin-10 and regulatory T-cells in cancer, *Curr. Opin. Oncol.* 25 (6) (2013) 637–645.
- [75] D.S. Shouval, A. Biswas, J.A. Goettel, K. McCann, E. Conaway, N.S. Redhu, I. D. Mascanfroni, Z. Al Adham, S. Lavoie, M. Ibourk, D.D. Nguyen, J.N. Samsom, J. C. Escher, R. Somech, B. Weiss, R. Beier, L.S. Conklin, C.L. Ebens, F.G. Santos, A. R. Ferreira, M. Sherlock, A.K. Bhan, W. Muller, J.R. Mora, F.J. Quintana, C. Klein, A.M. Muise, B.H. Horwitz, S.B. Snapper, Interleukin-10 receptor signaling in innate immune cells regulates mucosal immune tolerance and anti-inflammatory macrophage function, *Immunity* 40 (5) (2014) 706–719.
- [76] S. Chen, T. Yue, Z. Huang, J. Zhu, D. Bu, X. Wang, Y. Pan, Y. Liu, P. Wang, Inhibition of hydrogen sulfide synthesis reverses acquired resistance to 5-FU through miR-215-5p-EREG/TYMS axis in colon cancer cells, *Cancer Lett.* 466 (2019) 49–60.
- [77] C. Szabo, C. Coletta, C. Chao, K. Modis, B. Szczesny, A. Papapetropoulos, M. R. Hellmich, Tumor-derived hydrogen sulfide, produced by cystathionine-beta-synthase, stimulates bioenergetics, cell proliferation, and angiogenesis in colon cancer, *Proc. Natl. Acad. Sci. U. S. A.* 110 (30) (2013) 12474–12479.
- [78] M. Muller, F. Hansmann, D. Arnone, M. Choukour, N.C. Ndiaye, T. Kokten, R. Houlgatte, L. Peyrin-Biroulet, Genomic and molecular alterations in human inflammatory bowel disease-associated colorectal cancer, *Unit. Eur. Gastroenterol. Jpn.* 8 (6) (2020) 675–684.
- [79] D.E. Aust, J.P. Terdiman, R.F. Willenbacher, C.G. Chang, A. Molinaro-Clark, G. B. Baretton, U. Loehrs, F.M. Waldman, The APC/beta-catenin pathway in ulcerative colitis-related colorectal carcinomas: a mutational analysis, *Cancer* 94 (5) (2002) 1421–1427.
- [80] M. Michel, L. Kaps, A. Maderer, P.R. Galle, M. Moehler, The role of p53 dysfunction in colorectal cancer and its implication for therapy, *Cancers* 13 (10) (2021).